TECHNICAL RESEARCH REPORT

Simulator Development for a Spatially Controllable Chemical Vapor Deposition System

by Jae-Ouk Choo, Raymond A. Adomaitis, Gary W. Rubloff, Laurent Henn-Lecordier and Yijun Liu

TR 2002-49

hESimulator Development for a Spatially Controllable Chemical Vapor Deposition System

Jae-Ouk Choo[a], Raymond A. Adomaitis[a],*, Gary W. Rubloff[b], Laurent Henn-Lecordier[c] and
Yijun Liu[c]

[a] Department of Chemical Engineering and Institute for System Research,
University of Maryland, College Park, MD 20742, USA
[b] Department of Material and Nuclear Engineering and Institute for System Research,
University of Maryland, College Park, MD 20742, USA
[c] Institute for System Research,
University of Maryland, College Park, MD 20742, USA

* Corresponding author. Phone: (301) 405-2969, Fax: (301) 314-9920, Email: adomaiti@umd.edu

September 9, 2002

Abstract

Most conventional chemical vapor deposition systems do not have the spatial actuation and sensing capabilities necessary to control deposition uniformity, or to intentionally induce nonuniform deposition patterns for single-wafer combinatorial CVD experiments. In an effort to address this limitation, we began a research program at the University of Maryland focusing on the development of a novel CVD reactor system that can explicitly control the (2-dimensional) spatial profile of gas-phase chemical composition across the wafer surface. This reactor is based on a novel segmented showerhead design in which gas precursor composition can be individually controlled in the gas fed to each segment. Because the exhaust gas is recirculated up through the showerhead though the individual segments, the gas flow pattern created eliminates convective mass transfer between the segment regions. The effect of this design is a CVD system in which across-wafer composition gradients can be accurately predicted and controlled.

This paper discusses the development of a simulator for a three-segment prototype that has recently been constructed as a modification to an Ulvac ERA1000 CVD cluster tool. A preliminary set of experiments has been performed to evaluate the performance of the prototype in depositing tungsten films for a range of wafer/showerhead spacing and segment gas compositions. We discuss the simulation approach taken to developing the simulator for this system focusing on a one-dimensional simulation of transport through the segments and exhaust mixing region, a model valid in the limit of close showerhead/wafer spacing. The use of simulation in the prototype system design, interpreting experimental data, and its ultimate use in controlling the CVD process to achieve true programmable CVD operation all will be discussed. Further information can be found at the project website http://www.isr.umd.edu/Labs/CACSE/research/progrxr

1. Introduction

Chemical Vapor Deposition (CVD) is one of the essential processes in semiconductor manufacturing because of its ability to deposit thin smooth films conformally onto submicron-scale features. CVD processes have evolved together with the semiconductor industry, from early bell-jar CVD reactors to the current cold-wall single-wafer reactor [1]. Although current conventional CVD reactors produce thin smooth films successfully, their configurations lack of 2-dimensional spatial controllability of deposition to counteract non-uniformity generators such as reactant depletion. Significant research effort has been put into improving uniformity of deposited thin films [2]-[17]; most focus on optimizing the process parameters such as the gas feed rate, wafer temperature and reactor pressure in reactor configurations that do not allow any adjustments to their overall geometry [2]-[7][9]. Because current configurations of CVD reactors do not have precise control actuators for gas delivery to the wafer surface, optimization research is limited by in-flexible CVD reactor configurations. Some research has focused on distributing precursor gases across the wafer surface with pre-specified spatial variation [10]-[15]. A number of these studies are motivated by the goal of decreasing gas phase reactions in MOCVD processes using designs that separate precursors to improve film uniformity [11]-[15].

In our research, we have developed a novel CVD reactor design to improve 2-dimensional controllability. This CVD reactor includes a new segmented showerhead design featuring individually controllable gas distribution actuators, a design that reverses the residual gas flow, directing it up through the showerhead (henceforth referred to as the reverse-flow design) and sampling ports for in-situ gas sampling. In this paper, we describe the proof of this novel design concept by simulation and a sequence of experiments performed using a prototype reactor. We refer to this design as the Programmable CVD Reactor Concept because of the potential of real-time control of gas phase composition across the wafer surface. An illustration of this CVD reactor is shown in Figure 1.
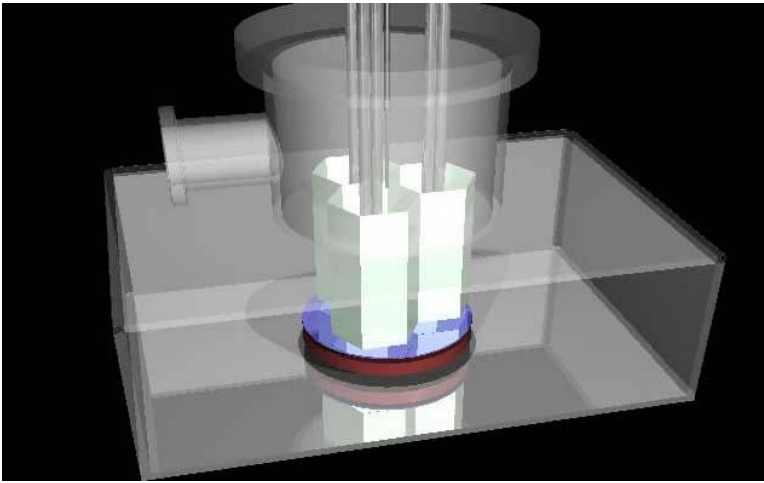
Figure 1. 3-D illustration of the Programmable CVD reactor.

2. CVD reactor design and prototype reactor

The major design feature of the Programmable CVD is its segmented showerhead. A schematic diagram of the reactor is shown in the figure below.
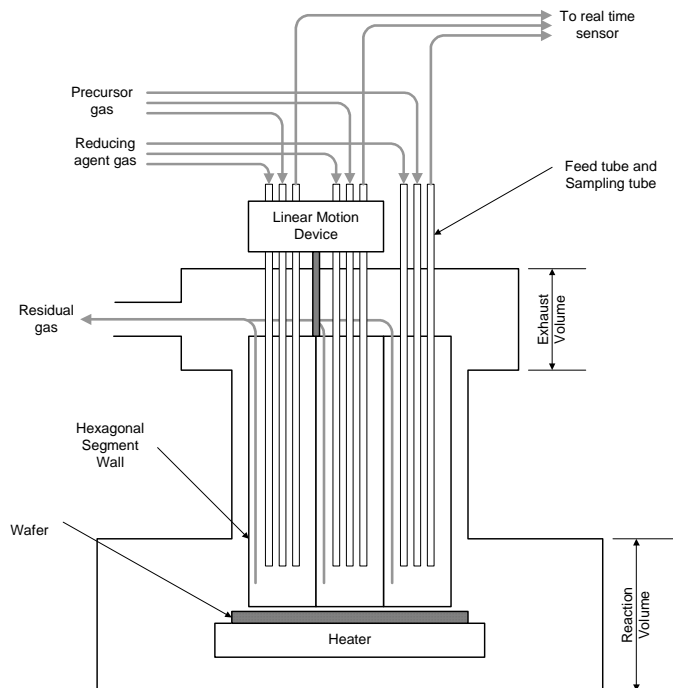

Figure 2. Schematic diagram showing a vertical cross-section of the Programmable CVD reactor.

2.1 Reactor design elements

The effect of the segmented showerhead design is to discretize the region above the wafer surface into individually controllable regions. Because each segment is fitted with separate feed gas lines, the precursor gas composition in the area of wafer surface corresponding to each segment can be individually adjusted.

To enhance film uniformity in the wafer area corresponding to each segment and to reduce interaction between each segment, residual gas is recirculated up through each segment of the showerhead and mixed in a common exhaust volume above the showerhead segments. This reverse-flow of exhaust gas means diffusional transport dominants in the region between the wafer and the bottom of the showerhead segments, increasing the controllability of across-wafer gas composition relative to conventional CVD reactor which normally draw residual gas across the wafer surface. Showerhead/wafer spacing is controlled with the linear motion device shown in Figure 2. The sampling tube of each segment carries a small amount of gas to a real time in-situ sensor, such as a mass spectrometer. From the residual gas analysis of each segment, approximate film thickness and the composition of film deposited on the wafer area corresponding to each segment can be determined. Also, this sampling tube and sensor can be used to diagnose process operation during a deposition run.

2.2 Prototype CVD reactor

To test the feasibility of the Programmable CVD concept, we have constructed a prototype reactor by modifying one reaction chamber of an Ulvac-ERA1000 CVD cluster tool. The Ulvac-ERA1000 CVD cluster tool located on the University of Maryland's campus is a commercial CVD tool used for selective tungsten deposition. In its original configuration, the hydrogen reducing gas entered through a quartz showerhead above the wafer; wafer heating was provided by a ring of heating lamps above the showerhead. As part of the programmable reactor modifications, substrate heating was used in place of lamp heating, and the quartz showerhead was replaced by a new assembly consisting of a three-segment honeycomb structure equipped with two feed tubes and one sampling tube per each segment. (See Figures 1 and 2.) With the prototype system, we performed blanket tungsten deposition experiments (at below 1torr and at 300-350°C wafer temperature) using hydrogen reduction; this deposition process was chosen to test the prototype reactor because the Ulvac reactor originally was designed for tungsten deposition, and the reactions

for tungsten deposition by hydrogen reduction have well known mechanisms and rate expressions [18]-[25]. Additionally tungsten deposition remains a commercially important manufacturing process [26][27].

3. Modeling and simulation

Significant effort was put into developing a process simulator for the prototype system, both to assess the effectiveness of the segment design and to determine the operating conditions for the initial set of experiments. Because of the Programmable CVD reactor's reverse-flow design, components of the gas mixture in the common exhaust volume can diffuse back into the segments. Therefore, to sustain the pre-specified gas compositions at the bottom of each segment, the back diffusion through the segment should be suppressed below an acceptable level by the convective upward flux contribution. A steady-state 1-dimensional segment model (for each segment) combined with a well-mixed common exhaust volume model was used to assess the ability of the segmented structure to maintain significant segment-to-segment gas composition differences near the wafer surface. The geometry of a single segment, together with the notation used in the model development, is shown in Figure 3. A schematic diagram of common exhaust volume is shown in Figure 4 where the each shaded area represents the top of the each segment of the showerhead.
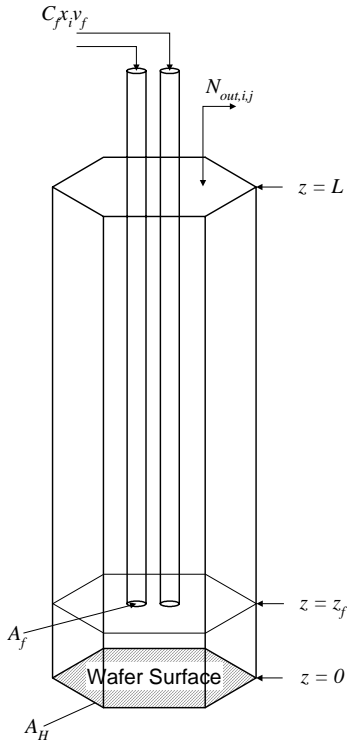
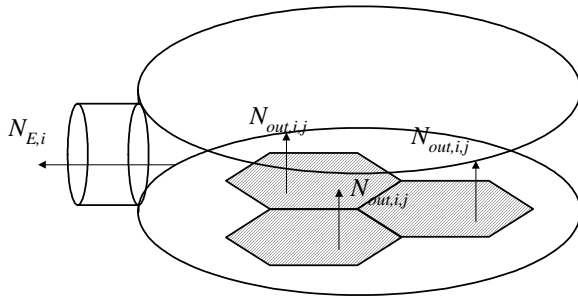Figure 3. Schematic diagram of a single showerhead segment.

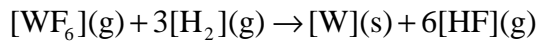Figure 4. Schematic diagram of the common exhaust volume.

3.1 Overall reaction and reaction rate expression

The overall reaction of tungsten deposition by hydrogen reduction is

$$[WF_6](g) + 3[H_2](g) \rightarrow [W](s) + 6[HF](g)$$

The gas phase reactions associated with this deposition process are negligible due to low reactor pressure during the process operation [18][21]. Surface reactions by Si reduction

will occur during the film nucleation step, but it will be neglected in the development of this steady-state deposition model. The overall reaction rate can be expressed as the following surface reaction expression,

$$R_{kin} = k_o[P_{WF_6}]^0[P_{H_2}]^{1/2} \exp\left(-\frac{E_a}{RT}\right)$$ (1)

For our simulations, the parameter values suggested by Kleijn et al are used [21]. ($k_o = 1.7$ [mol·Pa$^{-1/2}$·m^{-2}·s^{-1}] and $E_a = 69000 \sim 73000$ [J·mol^{-1}·K^{-1}]) According to this empirical model, the reaction rate does not depend on WF_6 partial pressure of when sufficient WF_6 is present [21][22].

3.2 Mass balance and transport of species.
In the limit of zero distance between the segment wall bottom and wafer surface, the mass balance for each species in each segment can be written as,

$$\frac{\partial Cx_i}{\partial t} = -\nabla N_i + F_i, \text{ where } i = 1,2,\dots,n.$$ (2)

Under the 1-dimensional steady-state assumption, (2) is rewritten as

$$N_i = \begin{cases} \alpha_i R_{kin} & (0 \le z \le z_f) \\ \alpha_i R_{kin} + C_f x_i v_f\left(\dfrac{A_f}{A_H}\right) & (z_f \le z \le L) \end{cases}$$ (3)

Because this CVD process takes place at low pressure, we can compute the value of total concentration using the ideal gas low [22]. Furthermore, the gas species transport can be expressed rigorously by the Stefan-Maxwell equation, the most rigorous expression for multi-species mixture transport, eliminating the need to calculate the multi-component diffusion coefficients, an approximation that often take significant amount of numerical effort because of the dependency on gas species concentration [22][28][29]. In our research, the binary diffusion coefficient is estimated by the Chapman-Enskog kinetic theory and Neufield method [22][30].
Neglecting any effect of pressure and forced diffusion, the Stefan-Maxwell equation can be written as

$$\nabla x_i = \sum_{j=1, j \neq i} \frac{1}{CD_{ij}} \left(x_i \overline{N}_j - x_j \overline{N}_i \right) \tag{4}$$

where $\overline{N}_i = N_i + \dfrac{\mathbf{D}_i^T}{M_i} \nabla \ln T$

Equation (4) can be rearranged into matrix form,

$$
\nabla
\begin{bmatrix}
x_1 \\
x_2 \\
\vdots \\
x_{n-1}
\end{bmatrix}
= \frac{1}{C}
\begin{bmatrix}
a_{1,1} & a_{1,2} & \cdots & a_{1,n-1} \\
a_{2,1} & \cdots & & \\
\vdots & & & \\
a_{n-1,1} & \cdots & & a_{n-1,n-1}
\end{bmatrix}
\begin{bmatrix}
x_1 \\
x_2 \\
\vdots \\
x_{n-1}
\end{bmatrix}
- \frac{1}{C}
\begin{bmatrix}
b_1 \\
b_2 \\
\vdots \\
b_{n-1}
\end{bmatrix}
\tag{5}
$$

where $a_{i,i} = \sum_{j=1, j \neq i}^{n} \left(\dfrac{\overline{N}_j}{D_{ij}} \right) + \dfrac{\overline{N}_i}{D_{in}}$

$$a_{i,j} = -\frac{\overline{N}_i}{D_{ij}} + \frac{\overline{N}_i}{D_{in}}$$

$$b_i = \frac{\overline{N}_i}{D_{in}}$$

Equation (5) then can be written as

$$\frac{d}{dz}\mathbf{x} = \frac{1}{C}\left[\mathbf{Ax} - \mathbf{b} \right] \tag{6}$$

The first step solving ordinary differential equation (6) is to estimate the gas composition at the bottom of each segment. Then, the flux of each gas species is determined by equation (1) and equation (3). Then equation (6) can be solved numerically by typical numerical ODE solver (recall the coefficients of A are not constant). The resulting solution then is compared to the boundary condition at the top of each segment. In the case (no mixing) that no interaction occurs between segments in the common exhaust volume, $d\mathbf{x}/dz$ should be zero at $z=L$. When the gases leaving each showerhead segment are mixed perfectly in the common exhaust volume, the mole fraction of each gas can be determined by following equations,

$$x_{i,j} = \frac{N_{out,i,j}}{\sum\limits_{i=1}^{n} N_{E,i}} \quad \text{at } z=L \quad \text{where} \quad N_{E,i} = \sum\limits_{j=1}^{ns} N_{out,i,j} \tag{7}$$

Thus, an iterative procedure is defined by which each segment composition profile is determined.

Because the temperature profile in the gas phase in the hexagonal segment is not currently well understood, we assume it takes the form of the linear temperature profile shown in Figure 5.
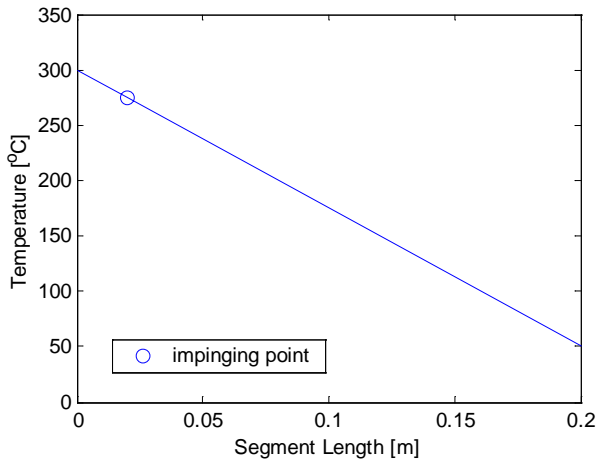

Figure 5. Temperature profile in a hexagonal segment along the z direction.

Simulations were performed using the gas feed recipes shown in Table 1. In Perfect Mixing cases1 and 2, the residual gases leaving each segment are mixed perfectly in the common exhaust volume. No mixing occurs inside the common exhaust region in the No Mixing case. The gas feed ratio of WF_6 and H_2 in segment 1 of each case was set to a typical process condition (1:4).

Case	No Mixing	Perfect Mixing 1			Perfect Mixing 2		
Segment	1,2,3	1	2	3	1	2	3
WF_6 mole fraction (%)	20	20	0	0	20	100	100
H_2 mole fraction (%)	80	80	100	100	80	0	0

Table 1. Gas feed recipes of each segment of three cases.

In Figure 6, the computed growth rates of tungsten film under segment 1 are shown.

According to the simulation results, the growth rates of each case all converge to a single value in the limit of very high gas feed flow rate. In the Perfect mixing 1 case, growth rate of tungsten film is higher than in the No Mixing case because H_2 gas leaving the other two segments diffuses back into segment 1. Similarly, in the Perfect Mixing 2 case, growth rate is lower than in the No Mixing case because the WF_6 diffusing from two other segments to segment 1 dilutes the H_2 (recall the film growth rate expression depends only on the partial pressure of H_2). As the feed gas flow rate increases, the convective flux contribution to the net flux of each species in the segments tends to reduce the back-diffusion of gas species found in the common exhaust region. Thus, at higher flow rates, a segment performs close to an ideally separated segment. According to our simulation results, the performance of the prototype will practically match the ideal, no-mixing case when the total gas flow to each segment is between 200 to 300 sccm, feed gas flow rate values which are in the feasible operating range of the prototype system.
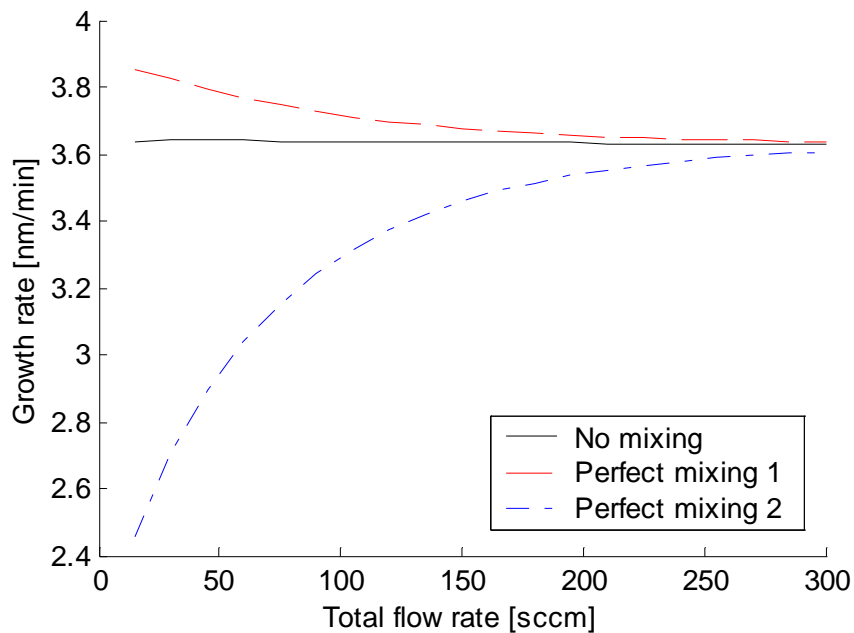

Figure 6. The simulation results of the Programmable reactor using the recipes shown in Table 1.

4. Experiment results

11

Preliminary experiments to assess the performance of the prototype system and to validate simulator predictions are underway. In one representative experiment, 45sccm H_2 and 15sccm WF_6 were fed to Segment 1, and 60sccm WF_6 and 60sccm H_2 were fed to Segments 2 and 3, respectively. Chamber pressure was maintained at 0.5torr, wafer temperature was set to $350^{o}C$, showerhead/wafer spacing was set to 2.5mm, and deposition took place during a 20 minute run. As can be seen in the image below, a wafer featuring three distinct deposition regions was produced, demonstrating proof of the concept that spatially patterned wafers can be produced in a CVD process by controlling across-wafer gas composition.

The film thickness in each segment region was determined by sheet resistance measurements using a four-point probe meter. The differences of thickness among the segment regions are in the expected range. The average film thicknesses are 0.473 μm, 0.287μm and 0.308μm in segment 1, 2 and 3, respectively.

Figure 7. Patterned tungsten film produced by the prototype Programmable CVD reactor.

5. Conclusion

A novel CVD reactor design was developed and a prototype reactor was constructed by modifying a commercial CVD reactor. Preliminary simulations and experimental testing of the feasibility of this new CVD reactor design concept were performed, demonstrating the effectiveness with which gas composition can be controlled across a wafer surface to produce an intentional, controlled pattern of film thickness nonuniformity. Continued experimental testing of the prototype Programmable CVD Reactor system is underway, along with the additional simulation studies necessary for assessing inter-segment diffusion near the wafer surface.

Acknowledgements

List of symbols

A_H, A_f	area [m^2]
C	total concentration [$mol \cdot m^{-3}$]
D	binary diffusion coefficient [$m^2 \cdot s^{-1}$]
$\mathbf{D}^T$	thermal diffusion coefficient [$g \cdot m^{-1} \cdot s^{-1}$]
E_a	activation energy [$J \cdot mol^{-1} \cdot K^{-1}$]
k_o	constant in reaction expression [$mol \cdot Pa^{-1/2} \cdot m^{-2} \cdot s^{-1}$]
L	length of segment [m]
M	molar weight [g]
N	molar flux [$mol \cdot m^{-2} \cdot s^{-1}$]
n	number of species
ns	number of segments
P	pressure [Pa]
R_{kin}	reaction rate [$mol \cdot m^{-2} \cdot s^{-1}$]

R	universal gas constant [J·mol^{-1}·K^{-1}]
T	temperature [K]
v	linear low rate [m·s]
x	mole fraction
z	rectangular coordinate [m]
α	Stoichiometric coefficient

References

[1] L. Xia, P.W. Lee, M. Chang, I. Latchford, P.K. Narwankar, R. Urdahl, 'Chapter 11. Chemical Vapor Depostion', *Handbook of Semiconductor Manufacturing Technology edited by Yoshi Nishi, Robert Doering*,New York: Marcel Dekker, 2000.

[2] C.A. Wang, S.H. Groves and S.C. Palmateer, Flow visualization studies for optimization of OMVPE preactor design, *Journal of Crystal Growth* **77**,136(1986)

[3] H.K. Moffat and K.F. Jensen, Three-dimensional flow effects in silicon CVD in horizontal reactor, *Journal of the Electrochemical society* **135**, 459(1988)

[4] C.R. Kleijn, Th.H. van der Meer, and C.J. Hoogendoorn, A mathematical model for LPCVD in a single wafer reactor, *Journal of the Electrochemical Society* **136**, 3423(1989)

[5] K.F. Jensen, Detailed models of the MOVPE process, *Journal of Crystal Growth* **107**, 1(1991)

[6] P.N. Gadgil, Optimization of a stagnation point flow reactor design for metalorganic chemical vapor deposition by flow visualization. *Journal of Crystal Growth* 134, 302(1993)

[7] B.M. Kim and Hong.H. Lee, Numerical simulation of metallorganic chemical vapor deposition of copper in a single-wafer reactor, *Journal of the Electrochemical Society* **144**, 1765(1997)

[8] K.J. Bachmann, H.T. Banks, C. Höpfner, G.M. Kepler, S. Lesure, S.D. McCall and J.S. Scroggs, Optimal design of a high pressure organometallic chemical vapor deposition reactor, *Mathematical and Computer Modeling* **29**, 65(1999)

[9] H. van Santen, C.R. Kleijn and H. E. A. van den Akker, On turbulent flows in cold-wall CVD reactors, *Journal of Crystal Growth* 212, 299(2000)

[10] M.M. Moslehi, C.J. Davis and R.T. Matthews, Programmable multizone gas injector for single-wafer semiconductor processing equipment, United State Patent #5,453,124. Sep. 26, 1995

[11] W. van der Stricht, I. Moerman, P. Demeester, J.A. Crawley and E.J. Thrush, Study of GaN and InGaN films grown by metaloganic chemical vapor deposition, *Journal of Crystal Growth* **170**, 344(1997)

[12] C. Yang, C. Huang, G. Chi and M. Wu, Growth and characterization of GaN by atmosphere pressure metalorganic chemical-vapor deposition with a novel separate-flow reactor, *Journal of Crystal Growth* **200**, 39(1999)

[13] C. Theodoropoulos, T.J. Mountziaris, H.K. Moffat and J. Han, Design of gas inlets for the growth of gallium nitride by metalorganic vapor phase epitaxy, *Journal of Crystal Growth* **217**, 65(2000)

[14] R.P. Pawlowski, C. Theodoropoulos, A.G. Salinger, T.J. Mountziaris, H.K. Moffat, J.N. Shadid, E.J. Thrush, Fundamental models of the metalorganic vapor-phase epitaxy of gallium nitride and their use in reactor design, *Journal of Crystal Growth* **221**, 622(2000)

[15] H.X. Wang, T. Wang, S. Mahanty, F. Komatsu, T. Inaoka, K. Nishino and S. Sakai, Growth of GaN layer by metal-organic chemical vapor deposition system with a novel three-flow reactor, *Journal of Crystal Growth* **218**, 148(2000)

[16] R. Walker, A.I. Gurary, C. Yuan, P. Zawadzki, K, Moy, T. Salagaj, A.G. Thompson, W.J. Kroll, R.A. Stall and N.E. Schumaker, Novel high temperature metal organic chemical vapor deposition vertical rotating-disk reactor with multizone heating for GaN and related materials, *Materials Science and Engineering B* **35**, 97(1995)

[17] J.D. Stuber, I. Trachtenberg and T. Edgar, Design and modeling of rapid thermal processing systems, *IEEE transaction on semiconductor manufacturing* **11**, 442(1998)

[18] R. Arora and R. Pollard, A Mathematical model for chemical vapor deposition process influenced by surface reaction kinetics: application to low-pressure deposition of tungsten, *Journal of the Electrochemical Society* **138**(5) 1523(1991)

[19] J.J. Hsieh, Influence of surface-activated reaction kinetics on low-pressure chemical vapor deposition conformality over micro feature, *Journal of the Vacuum Science and Technology A* **11,** 78(1993)

[20] C.R. Kleijn, Computational modeling of transport phenomena and detailed chemistry in chemical vapor deposition – a benchmark solution, *Thin Solid Films* **365**, 294

(2000)

[21] C.R. Kleijn, C.J. Hoogendoorn, A. Hasper, J. Holleman and J. Middelhoek, Thransport phenomena in tungsten LPCVD in a single-wafer reactor, *Journal of the Electrochemical Society* **138**, 509(1991)

[22] C.R. Kleijn and C. Werner, *Modeling of chemical vapor deposition of tungsten films*, Basel; Boston: Birkhäuser Verlag, 1993

[23] K.J. Kuijlaars, C.R. Kleijn and H.E.A. van den Akker, A detailed model for low-pressure CVD of tungsten, *Thin Solid Films* **270**, 456(1995)

[24] C.M. McConia and K. Krishnamani, The kinetics of LPCVD tungsten deposition in a single wafer reactor, *Solid State Science* **133**, 2542 (1986)

[25] P. Van Der Putte, The reaction kinetics of the H_2 reduction of WF_6 in the chemical vapor deposition of tungsten films, *Philips Journal of Research* **42**, 608 (1987)

[26] P.J. Ireland, High aspect ratio contacts: A review of the current tungsten plug process, *Thin Solid Films* **304**, 1(1997)

[27] J. Baliga and S. Crum, Interconnection Today, *Semiconductor International*, September (2000)

[28] J.C. Slattery, *Advanced Transport Phenomena*, Cambridge, UK; New York, NY: Cambridge University Press, 1999.

[29] R.B. Bird, W.E. Stewart and E.N. Lightfoot, *Transport phenomena*, New York: John Wiley and Sons, 1960.

[30] R.C. Reid, J.M. Praunitz and B.E. Poling, The properties of gases and liquids (4th edition), New York, McGraw-Hill, 1987.